THE JOURNAL OF PHYSICAL CHEMISTRY B

Article

pubs.acs.org/JPCB

Correlation of Structural Order, Anomalous Density, and Hydrogen Bonding Network of Liquid Water

Dibyendu Bandyopadhyay,[†] S. Mohan,[†] S. K. Ghosh,[‡] and Niharendu Choudhury*[,‡]

[†]Heavy Water Division, [‡]Theoretical Chemistry Section, Bhabha Atomic Research Centre, Mumbai 400 085, India

ABSTRACT: We use extensive molecular dynamics simulations employing different state-of-the-art force fields to find a common framework for comparing structural orders and density anomalies as obtained from different water models. It is found that the average number of hydrogen bonds correlates well with various order parameters as well as the temperature of maximum densities across the different models, unifying apparently disparate results from different models and emphasizing the importance of hydrogen bonding in determining anomalous properties and the structure of water. A deeper insight into the hydrogen bond network of water reveals that the solvation shell of a water molecule can be defined by considering only those neighbors that are hydrogen-bonded to it. On the basis of this view, the origin of the appearance of a non-tetrahedral peak at a higher temperature in the distribution of tetrahedral order parameters has been explained. It is found that a neighbor that is hydrogen-bonded to the central molecule is tetrahedrally coordinated even at higher temperatures. The non-tetrahedral peak at a higher temperature arises due to the strained orientation of the neighbors that are non-hydrogen-bonded to the central molecule. With the new definition of the solvation shell, liquid water can be viewed as an instantaneously changing random hydrogen-bonded network consisting of differently coordinated hydrogen-bonded molecules with their distinct solvation shells. The variation of the composition of these hydrogen-bonded molecules against temperature accounts for the density anomaly without introducing the concept of large-scale structural polyamorphism in water.

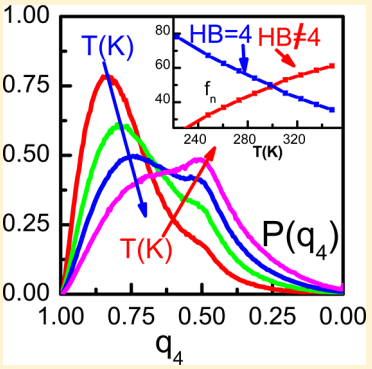

INTRODUCTION

Water, one of the most ubiquitous and abundant materials on earth, has a central importance in most of the chemical and biological processes.[1] The small molecular size, high dielectric constant, strong electrostatic interactions, high diffusivity, and ability to manifest hydrophobic interaction among hydrophobic groups present in it make it different from all other liquids and can be held responsible[2−4] for its remarkable ability to dissolve or stabilize varieties of solutes including proteins, nucleic acids, lipids, etc. In chemical and biological processes, solvent plays a very important role in deciding a solute's structural stability and its chemical and biophysical activities. The solvation process is basically controlled by the interaction of the solvent molecules with the solutes. Because of its extended hydrogen-bonded network structure, water is different from many simple liquids.

Water is an intriguing liquid not only because it has a completely different open tetrahedral local structure as compared to a closed packed local structure of a simple liquid but also due to its number of anomalous properties.[5−10] It is believed that a relationship exists between the local structure and the anomalous properties of water. A large number of studies[11−17] has been devoted to understand this relationship by using atomistic models of water. Different groups have used different models of water and have come up with seemingly disparate results. Three-site models, because of their simplicity and less computational demand, are extensively used in biomolecular simulation. Four- and five-site models being more detailed yield better results as compared to the three-site models but at the cost of the computational economy associated with the three-site models. However, their accuracy in reproducing properties of water is not directly linked to the microscopic details of the molecular description in the model. For example, results obtained from four-site models such as TIP4P/2005[18,19] and TIP4P-Ew[20] are better than those obtained from a more involved five-site TIP5P[21] model. Although local structural order as predicted by radial distribution function or structure factor $S(Q)$, which can be obtained experimentally, has a direct connection[22] to many of the properties of water, analyses of these structural correlations do not provide any direct clue to understand the anomalies of water. This problem is further compounded by apparently disparate results for structural, thermodynamic, and density anomalies obtained from these models.[23] Therefore, one of the major hurdles in this direction is the nonexistence of a common framework to compare these apparently disparate results obtained from different water models. Efforts in this direction have been made, and it has been observed[23] that water properties are temperature-shifted for different models. In order to understand the structure and anomalies of water better, a direct relation between the structure forming capabilities of all these models and the density anomaly of water has to be established. To achieve this aim, in the present work, we compare various local orders and anomalies of water as obtained from different water models by identifying a key

Received: May 6, 2013
Revised: June 21, 2013
Published: July 16, 2013

   dx.doi.org/10.1021/jp404478y | *J. Phys. Chem. B* 2013, 117, 8831−8843

structural parameter that governs properties of water and therefore reconciles disparate findings obtained from different models.

As has already been mentioned, water has a number of anomalies and the best known of all these anomalies is the density anomaly, in which the average bulk density of water shows a maximum at around 4 °C at ambient pressure. Despite many efforts,[11−35] a simple and comprehensive explanation for the anomalies of water is still lacking. Even in recent past, it was intensely argued on the nature of the local structural motif of liquid water. A long-standing view emerged[36] from X-ray and neutron scattering experiments, thermodynamics data, and molecular simulations has interpreted liquid water in terms of a locally tetrahedral liquid structure, where a water molecule is H-bonded on average to four nearest neighbors. This traditional view was recently challenged by Wernet et al.,[37] who showed using X-ray Raman and absorption spectroscopy along with theoretical calculation that the structure of the first coordination shell in liquid water is not tetrahedral. Instead, they claimed that room temperature liquid water consists of a large fraction (98%) of broken H bonds and on average each water molecule is associated with only two strong H bonds. However, this view has been strongly contended by many groups.[38−41] By using state-of-the-art experimental techniques and atomistic and ab initio molecular dynamics simulations, these groups have reestablished[30,38−42] the traditional picture that water is a tetrahedral hydrogen-bonded network with some broken bonds.

Many people have tried to find out a universal relationship between the density and structure of water, primarily because the relation is fundamental to the understanding of water's anomalous properties and also due to the existence of varieties of structures in ice. The most important of the several hypotheses[24,25] proposed in recent literature is the liquid−liquid critical point view, according to which in the supercooled region water has a metastable critical point associated with a first-order phase transition between high-density-liquid (HDL) and low-density-liquid (LDL) phases. By extending this hypothesis into the ambient region, water's anomalous properties can be interpreted as an interplay between the structurally different HDL and LDL phases of water. In fact, in a recent experimental investigation, Huang et al.,[28] based on their analysis of $S(Q)$ data at low Q region, have proposed that extended clusters of HDL and LDL are present even under ambient conditions. This inference has been drawn on the basis of observed enhancement of $S(Q)$ in the low Q region and has been interpreted in terms of density fluctuations of two structurally distinct clusters of different densities. However, this view has been strongly debated by many groups.[16,29−31] Matsumoto[16] has found that two opposing linear correlations, normal thermal expansion against temperature and contraction due to angular distortion, are responsible for the density anomaly of water without invoking structural heterogeneity. Clark et al.[29] and Soper et al.[30] have shown that the enhancement of $S(Q)$ at small angle (i.e., small Q) is a consequence of normal density fluctuations of the stochastic processes present in a single component fluid. Their simulation of TIP4P-Ew water has shown no bimodality in the density histogram in the length scales ranging from 0.6 to 6 nm and thus emphasizes the fact that enhancement of $S(Q)$ at low Q is not due to coexistence of two different local structural motifs in liquid water under ambient conditions. It has been demonstrated further by Sedlmeier et al.[31] that there are only small spatial correlations between local density and structural fluctuations, indicating no direct connection between density−density correlation and spatial correlation of structure in liquid water. Poole and co-workers[32] and Tse and co-workers,[33] although have found mixture-like behavior and density fluctuation in supercooled water, no density inhomogeneity has been observed[33] in water under ambient conditions. In a very recent simulation study, Limmer et al.[43] have explored the free energy landscape of water for a range of temperatures and pressures including state points where amorphous behavior is unstable with respect to the crystal. They could not find more than a single liquid basin in the entire range of temperatures and pressures and thereby excluded the possibility of the proposed liquid−liquid critical points. However, in support of the findings of Huang et al.,[28] very recently Patey and co-workers[34] have shown that, if water can be considered as a mixture of two species having different local angular arrangements as measured by the tetrahedral order parameter, considerable concentration fluctuations can occur even at ambient condition and this concentration fluctuation correlates with density fluctuation, providing support and explanation of the notion of structural polyamorphism in water.

However, this analysis[34] is based solely on considering water as a mixture of two different kinds of molecular arrangements distinguished entirely by the tetrahedral order parameter, q_i, a quantity used to estimate the extent of tetrahedrality in a water molecule i. The median value of q_i has been used as a demarcation between two structurally different local motifs, one with more and another with less orientationally ordered structures. Therefore, the underlying assumption is that all the water molecules having q_i values less than the median have the same fixed local structure, which is structurally distinct from the structural motif of a water molecule with q_i value above the median. However, the local structure and hence the tetrahedral order parameter q_i of a molecule is changing at every instant of time, and moreover, the median of the q_i values changes with temperature. Therefore, the ensemble average of these instantaneously changing orientational arrangements may not lead to a description of water as a mixture of two different structurally distinct entities. Moreover, unless we know explicitly about the origin of a particular q_i value, i.e., what local structural arrangement corresponds to what q_i value, it is very difficult to conceive water as a mixture of two structural arrangements even temporally. It is well-known[30] that, at a low enough temperature, the distribution of q values is unimodal with a single peak at around q = 0.83, suggesting almost tetrahedral arrangements of the four neighbors of a central molecule. As we increase the temperature, a new peak appears at an intermediate q value of around 0.5. No clear explanation of this low-q peak is available in the literature. A deeper insight[35] into the origin of the low-q peak in the distribution of tetrahedral order parameters and its relation with water's local structure is therefore essential to understand the relation of this local order (as represented by the q value) with local structural motifs of water. In the present investigation, we therefore intend to focus our attention on correlating local hydrogen bonding structure with different structural orders and density anomaly of water. In the process, we analyze the origin of the low-q peak in the distribution of tetrahedral order parameters, i.e., the correspondence of the low-q peak to the local structural motif. The present study based on computer simulations of various models of water suggests that water can be viewed as a dynamical mixture of distinctly different solvation shells of

dx.doi.org/10.1021/jp404478y | J. Phys. Chem. B 2013, 117, 8831−8843

Table 1. Temperature Range and TMD of All the Water Models

model	SPC/E	SPC	TIP3P	TIP4P	TIP4P/2005	TIP5P
temperature range (K)	223−373	200−373	150−373	223−360	246−370	260−348
TMD (K)	240	221	200	260.5	285	285
$\langle n_{HB} \rangle$ at TMD	3.76	3.75	3.74	3.68	3.69	3.38
q_4	0.715	0.716	0.692	0.694	0.691	0.689
Q_6	0.271	0.270	0.268	0.270	0.269	0.271

differently (two-, three-, four-, five-) hydrogen-bonded molecules. By taking into consideration the void space between the first and second shells of water, the density anomaly can then be nicely interpreted in terms of the change in composition of this mixture with the change in temperature without incorporating the idea of large length scale structural polyamorphism.

MODELS AND METHODS

In the present investigation, we have used six different rigid body atomistic models of water having fixed bond lengths and bond angles. These are TIP3P,[44,45] SPC,[46] SPC/E,[47] TIP4P, TIP5P,[21] and TIP4P/2005.[18] In each of these models, only the oxygen atom is considered to be a Lennard-Jones (LJ) interaction site and the partial charges are distributed on atomic sites as well as virtual sites in some of the cases.

For all the simulations, we have used 512 water molecules placed in a cubic box. The simulations were performed in the NPT ensemble with the molecular dynamics extended system approach of Nose and Anderson.[48] Periodic boundary conditions and minimum image convention were used in all three directions. For all three site models, the bonds and the angle of a water molecule were constrained by fixing two bonds and HH distance using the RATLE algorithm and the Ewald method was adopted for treating electrostatic interactions. Equations of motion were integrated using the velocity Verlet algorithm with a time step of 2 fs. For four- and five-site models, we have used the GROMACS[49] simulation program with the PME method for electrostatics. All the simulations were carried out at a target pressure of 1 atm at a number of target temperatures, the range of which for each model is shown in Table 1. For simulations at temperatures of 285 K and below, the first 10 ns was discarded for equilibration and trajectories for the next 10 ns have been stored for analyses, whereas, for state points with a temperature of 285 K and above, the first 3 ns was discarded for achieving equilibrium and the next 5 ns runs have been stored for analyses.

Local Orders. Ice has an almost perfect three-dimensional hydrogen-bonded network with tetrahedral arrangements. For a perfectly tetrahedral ice-like structure, there are 4 nearest neighbors around a central water molecule in the first shell and another 12 neighbors in the second shell. Unlike ice, in bulk water, there are broken hydrogen bonds due to randomness introduced by thermal energy and therefore perfect tetrahedral local order is not maintained. In order to measure the magnitude of oriental order in liquid water, two different orientational order parameters[11,15] for first and second shells have been used here.

(1). Tetrahedral Order Parameter. The tetrahedral order parameter, q_i, used to define the extent of tetrahedrality of the local water structure involving four molecules in the first shell of a central water molecule i is defined as

$$q_i = 1 - \frac{3}{8}\sum_{j=1}^{3}\sum_{k=j+1}^{4}\left[\cos\theta_{jik} + \frac{1}{3}\right]^2 \quad (1)$$

where θ_{jik} is the angle formed by neighbors j and k with the central molecule i. The average value of the tetrahedral order parameter averaged over all the molecules N is then defined as

$$q_4 = \frac{1}{N}\left\langle \sum_{i=1}^{N} q_i \right\rangle \quad (2)$$

It quantifies the tetrahedral order of the system by measuring the deviation from ideal tetrahedral structure. In the above equation, angular brackets $\langle\ \rangle$ represent an ensemble average. The equation is being formulated in such a way that the value of q_4 varies in the range 0−1. When the central water molecule is located at the center of a perfect tetrahedron with four nearest neighbors occupying the four vertices, values of $\cos\theta$ should be −1/3 and in that case q_4 is equal to 1 (see eq 1). For a perfectly random orientation, six angles formed by the combinations of any two of the four neighbors with the central molecule are independent of each other. In this case, the value of the constant term in eq 1 can be obtained[11] from angular averaging of each of the terms in the summation, viz., $(\int_0^\pi[\cos\theta + (1/3)]^2 \sin\theta\, d\theta)/(\int_0^\pi \sin\theta\, d\theta) = 4/9$. In order to get a q_i value of zero for the random uncorrelated orientations, the normalization constant of 3/8 before the summation in eq 1 arises from the contributions of six angles as $1/(6 \times 4/9)$ as used by Errington and Debenedetti.[11] In the present investigation, apart from using four neighbors, we would like to calculate the tetrahedral order parameter for a central molecule with two and three (H-bonded) neighbors as well. Thereby, the numbers of combined angles associated with a central molecule having three and two neighbors are three and one, respectively. Accordingly, we have used modified normalization constants of 3/4 [i.e., $1/(3 \times 4/9)$] for a central molecule with three neighbors and 9/4 [i.e., $1/(1 \times 4/9)$] for a central molecule with two neighbors so that the tetrahedral order varies between 1 (perfectly tetrahedral) and 0 (uncorrelated random configuration).

(2). Orientational Order Parameter for the Second Shell. Although the first shell of a water molecule in ice is almost tetrahedral, the second shell of the hexagonal ice crystal forms an hcp lattice. In order to characterize the angular orientation of the second shell molecules around a central water molecule, another order parameter Q_{6i} is generally used. It measures the angular preference of the 12 second-shell neighbors with respect to a central molecule toward fcc, bcc, or hcp structures. In order to compute this quantity, 12 hypothetical bonds connecting each of the 12 s-shell neighbors and the central molecule are assigned and for each bond its azimuthal and polar angles (θ, ϕ) are computed. Then, the average of the spherical harmonics $\overline{Y}_{lm}(\theta, \phi)$ over all 12 bonds of the central molecule i

dx.doi.org/10.1021/jp404478y | J. Phys. Chem. B 2013, 117, 8831−8843

is calculated, and from the average spherical harmonics, the function

$$Q_{li} = \left[\frac{4\pi}{2l+1} \sum_{m=-l}^{m=l} |\overline{Y_{lm}}|^2 \right]^{1/2} \quad (3)$$

is then calculated.[15] For $l = 6$, the average value of the orientational order parameter Q_6 for N molecules is calculated from the equation

$$Q_6 = \frac{1}{N} \sum_{i=1}^{N} Q_{6i} \quad (4)$$

The value of Q_6 is large for most crystals; for example, it is 0.574 for fcc, 0.511 for bcc, and 0.485 for hcp structures, and for uncorrelated systems, $Q_6 = 0.289$.

(3). Hydrogen Bond. Along with the above-mentioned orientational order parameters, the number of hydrogen bonds, n_{HB}, a water molecule forms with its neighbors, is considered as an alternative order parameter to measure the extent of the local arrangement of water molecules. The geometrical definition of the hydrogen bond is being adopted throughout this study. It takes into account both intermolecular separation, which is missing in the case of orientation order parameters, and associated angles involving oxygen as well as hydrogen atoms of two hydrogen-bonded water molecules. Thus, in our view, it carries a detailed description of the first shell than coordination number or q_i of a central molecule. According to the geometric criteria, two water molecules are considered to be H-bonded only if the interoxygen distance is less than 3.5 Å and simultaneously the hydrogen−oxygen (H-bonded) distance is less than 2.45 Å along with the H−O···O angle being less than 30°. Although the minima of the oxygen−oxygen radial distribution function (RDF) varies with temperature from around 3.2 to 3.75 in the temperature range studied here, we have chosen the oxygen−oxygen distance to be 3.5 Å in all the cases as the change in OO distance has a negligible effect on the average number of hydrogen bonds.

RESULTS AND DISCUSSION

Two order parameters frequently used in analyzing water structure are the tetrahedral order parameter, q_4, calculated from the angles made by any two of the four nearest neighbor molecules to the central molecule and the orientational order parameter Q_6, which measures angular arrangements of the second shell neighboring molecules with respect to the central molecule. These two order parameters along with radial distribution functions provide angular and spatial correlations of water. In order to investigate the temperature dependence of local structural order in water, we have calculated the tetrahedral order parameter q_4 and the orientational order parameter Q_6 as defined by eqs 2 and 4, respectively, for six different water models, namely, SPC, SPC/E. TIP3P, TIP4P, TIP4P/2005, and TIP5P. The temperature dependence of these two order parameters along the $P = 1$ atm isobar for different water models is shown in Figure 1a and b, respectively. Although all the models follow the same general trend that the order parameters monotonically decrease with the elevation of temperature, at a particular temperature, values of the order parameters obtained from different water models are quite different. It is important to note that different water models differ from each other in molecular geometry and intermolecular potential parameters, resulting in significantly different

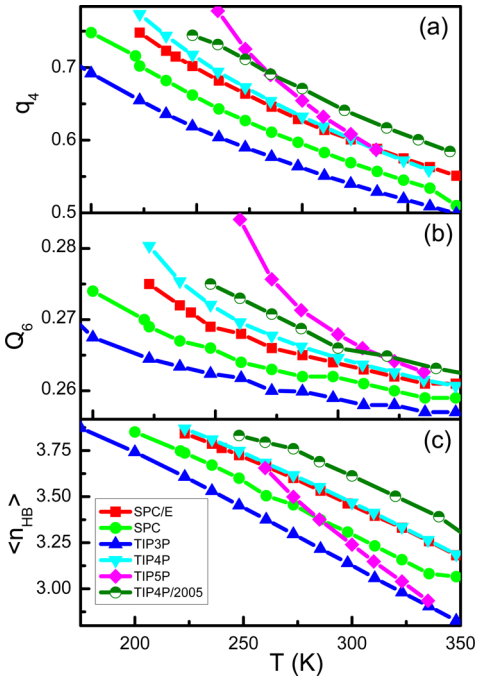

Figure 1. Average values of (a) the tetrahedral order parameter, q_4, (b) the orientational order parameter, Q_6, for the second shell water molecules, and (c) the number of hydrogen bonds as a function of temperature for different models of water.

hydrogen bonding network structure, and it is evident from the plots in Figure 1c that the temperature dependence of the average number of H-bonds, $\langle n_{HB} \rangle$, for different water models is quite different. At a particular temperature, different models yield different $\langle n_{HB} \rangle$. Therefore, it can be expected that nonequivalence of average numbers of hydrogen bonds obtained from different models could be the reason for the disparate structural orders shown in Figure 1a and b. We therefore intend to verify whether $\langle n_{HB} \rangle$ can be considered as a key parameter to reconcile apparently disparate temperature trends of the properties of water obtained from different water models.

Since both q_4 and Q_6 are related to mutual angular arrangements of water molecules, there may exist a correlation between the orientational order parameter and $\langle n_{HB} \rangle$, which is also dependent on the mutual orientation and distance between two molecules. Indeed, when these two order parameters are represented as a function of $\langle n_{HB} \rangle$, except for the TIP5P water model, all other models yield strikingly similar results (see Figure 2a and b for q_4 and Q_6, respectively). It signifies the existence of a relationship between the orientation order parameter and the H-bonding network structure of water over a wide range of temperatures. Existence of such a correlation is not so surprising in the case of q_4, because it is calculated by considering four nearest neighbors, the majority of which are hydrogen-bonded to the central molecule. However, the nice correlation observed between Q_6 and $\langle n_{HB} \rangle$ (see Figure 2b) is a bit surprising, as Q_6 is calculated based on the angular arrangements of the water molecules in the second shell with respect to a central molecule. It is probably because a molecule in the second shell is connected to that in the first shell through hydrogen bonding, for which a specific relative angular arrangement between the two water molecules from these two shells are required and, thus, the orientation of the second

dx.doi.org/10.1021/jp404478y | J. Phys. Chem. B 2013, 117, 8831−8843

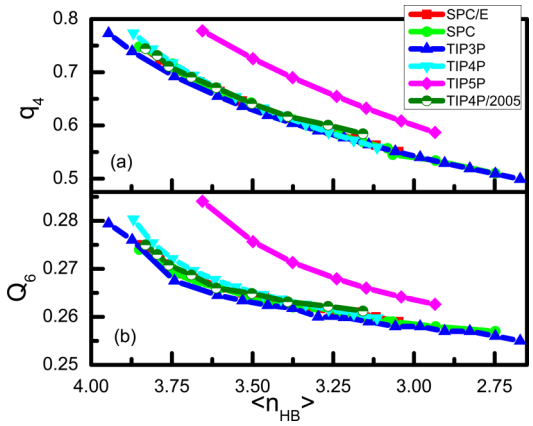

Figure 2. Average values of (a) the tetrahedral order parameter, q_4, and (b) the orientational order parameter, Q_6, as a function of the average number of hydrogen bonds, $\langle n_{HB}\rangle$, for different models of water.

shell molecules is indirectly influenced by the orientation of the first shell water molecules, based on which q_4 has been calculated.

Unlike q_4, Q_6, or $\langle n_{HB}\rangle$, each of which decreases steadily with the increase of temperature, the average density of water as a function of temperature passes through a maximum. When the bulk average density of water is plotted as a function of temperature, it is found (see Figure 3a) that results from

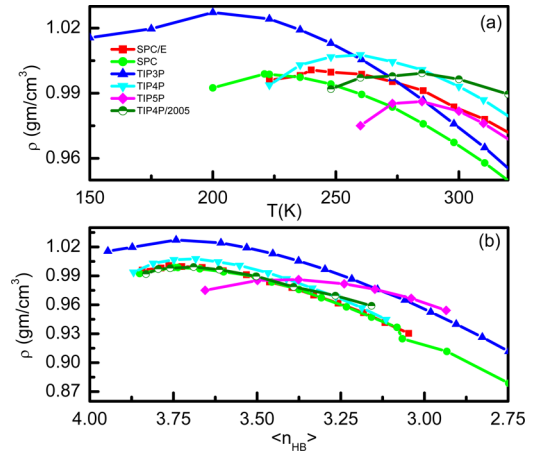

Figure 3. Average density of water for different water models as a function of (a) temperature and (b) average number of hydrogen bonds.

different water models are significantly different. In particular, locations of temperature of maximum density (TMD) (see Table 1) obtained from different water models are considerably different. However, when the densities from these different models are plotted as a function of $\langle n_{HB}\rangle$ in Figure 3b, we found[50] data from all the models except TIP5P to be almost coinciding, forming a master curve (although the plot of the TIP3P model is slightly up-shifted, the location of the TMD coincides with other models). The concurrent density peaks signify that the state corresponding to the TMD possesses a unique value of $\langle n_{HB}\rangle$ irrespective of the models used. The values listed in Table 1 in fact reveal that TMD of any water model is associated with a fixed number of hydrogen bonds, $\langle n_{HB}\rangle \approx 3.7$, and more interestingly, water has a specific orientational preference, as indicated by almost the same values of q_4 and Q_6 at their respective TMDs irrespective of the water models used. The TIP5P water model deviates considerably from the master curve formed by all other models. The problem related to the TIP5P water model is well-known in the literature,[23,51] and it is probably because of the increased preference for TIP5P water molecules to act both as tetrahedral hydrogen bond donors and acceptors.[51] It is also interesting to observe that the slope of the $\langle n_{HB}\rangle$ vs T plot for the TIP5P model (see the magenta line in Figure 1c) is quite different from that of any other model.

In order to check the correlation of $\langle n_{HB}\rangle$ with the distribution of the tetrahedral order parameter, $P(q_4)$, we have shown the calculated results in Figure 4a. We have chosen a low-temperature region (which is below the TMD) and a high temperature region (which is above the TMD) for each model, and the temperature for each model is chosen in such a way that the value of $\langle n_{HB}\rangle$ remains almost the same for whatever water model we use. In the low temperature region, the expected trend of unimodal distribution with a peak at a high q_4 value has been observed and different models yield identical distributions if values of $\langle n_{HB}\rangle$ are the same (see that the lines of blue, navy, cyan, and violet colors are almost overlapping). In the high temperature region, a much broader bimodal distribution has been observed and distributions obtained from different water models yield again an almost coinciding distribution if the average number of hydrogen bonds is the same (see all the curves with red, orange, pink, and red colors). Thus, it illustrates the uniqueness of tetrahedral angular distribution obtained from different water models if viewed as a function of $\langle n_{HB}\rangle$. Similar results have been obtained in previous investigations.[23,28] Besides the distribution of q_4, that of Q_6, i.e., $P(Q_6)$, also follows the same general trend (not shown here). Another important quantity related to water structure is the structure factor $s(k)$. In order to further check the validity of $\langle n_{HB}\rangle$ as a key parameter to correlate results from different models, we present in Figure 4b and c $s(k)$ obtained from different water models. Like the $P(q_4)$ vs q_4 plot, here too we have shown results for a low temperature region (Figure 4b) and a high temperature region (Figure 4c). The $s(k)$ values from different water models are exactly overlapping with each other if the values of $\langle n_{HB}\rangle$ are almost the same in both temperature regions.

All these observations confirm the existence of a correlation between the hydrogen bonding network of water and orientational order parameters as well as average density. This correlation makes one interested to analyze the local hydrogen bonding structure of water in a greater detail. Since we have shown the uniqueness of various structural orders and densities obtained from different models as a function of the average number of hydrogen bonds, $\langle n_{HB}\rangle$, now we can choose any one model for further detailed investigation and we have chosen the well-studied SPC/E model for that. Unlike in the crystalline state, where almost all the molecules are four hydrogen-bonded, in liquid water, a molecule can form n number of hydrogen bonds, where n varies from 1 to 6. Therefore, the average number of hydrogen bonds, $\langle n_{HB}\rangle$, at a particular temperature has contributions from all n-hydrogen-bonded molecules with n = 1−6. In Figure 5a, we have shown the percentage of n-hydrogen-bonded molecules as a function of temperature. It is seen that four-hydrogen-bonded molecules dominate at the lower temperature region. Elevation of temperature leads to an increase of two- and three-hydrogen-

dx.doi.org/10.1021/jp404478y | J. Phys. Chem. B 2013, 117, 8831−8843

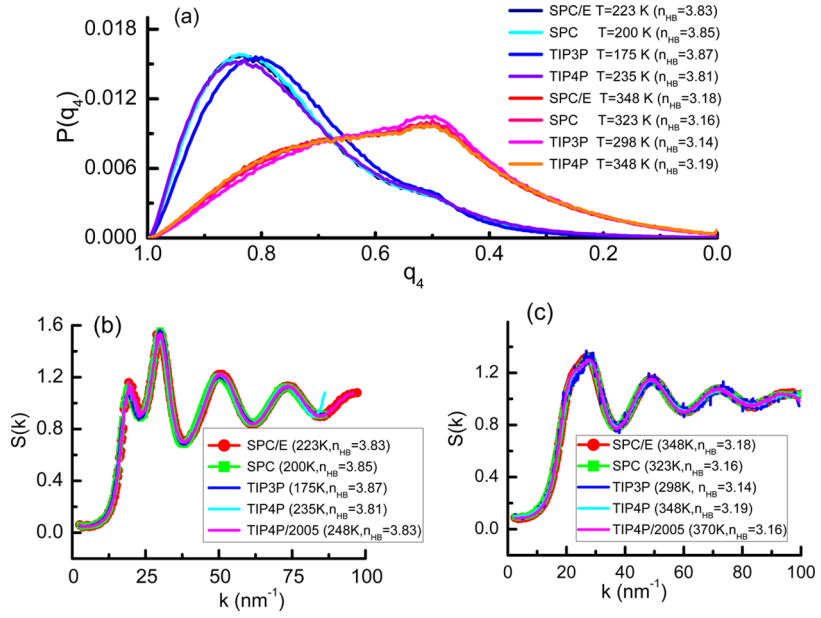

Figure 4. (a) Probability distribution $P(q_4)$ of the tetrahedral order parameter, q_4, for different water models. Distributions at lower temperatures for systems with almost the same $\langle n_{HB} \rangle$ in the range 3.81−3.87 (shown by lines with blue, violet, navy, and cyan colors) as obtained from different water models are almost overlapping. Similarly, those at higher temperatures for systems with almost the same $\langle n_{HB} \rangle$ in the range 3.14−3.19 (shown by lines with red, pink, magenta, and orange colors) also have similar distributions irrespective of the water model used. Static structure factors obtained from different water models (b) in the low temperature region and (c) high temperature region with almost the same number of average hydrogen bonds in each case.

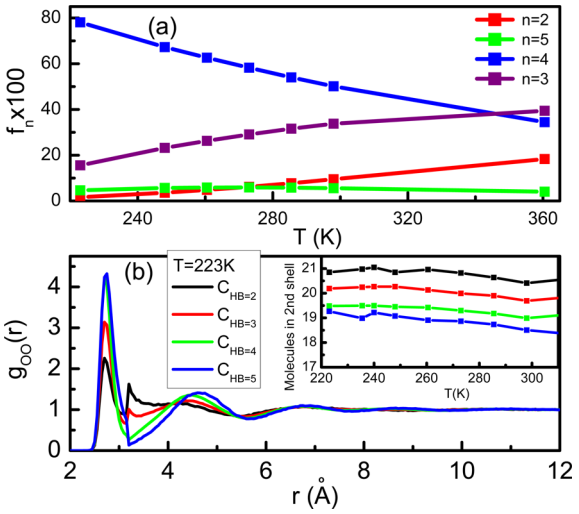

Figure 5. (a) Percentage of water molecules having n hydrogen bonds as a function of temperature and (b) radial distribution functions of water molecules around a central water molecule having n hydrogen bonds, i.e., $C_{HB=n}$ with n = 2−5 at T = 223 K. In the inset, the number of water molecules in the second solvation shell as obtained from the integration of the radial distribution function has been shown as a function of temperature.

bonded molecules but a decrease of four-hydrogen-bonded molecules. There is very little change in the percentage of the five-hydrogen-bonded molecules in the entire temperature range. Henceforth, we use $C_{HB=n}$ to designate a central molecule, which forms n-hydrogen bonds with the neighboring molecules. For example, $C_{HB=2}$ represents a water molecule having only two hydrogen bonds with the neighboring molecules and so on. It has been found that the percentage of $C_{HB=n}$ with n = 1 as well as 6 (or more) is very less and can be ignored for further analyses. Thus, we shall confine our attention to the cases of $C_{HB=n}$, with n = 2−5. To form a hydrogen bond, certain geometrical criteria involving distance and angle need to be fulfilled. However, in the case of orientational order parameters (q_4 or Q_6), we select a fixed number of nearest neighbors, viz., 1st to 4th nearest neighbors in the case of q_4 and 5th to 16th molecules (distance wise) for Q_6 calculations around a central molecule, irrespective of the relative distance and orientation of each of these neighboring molecules with respect to the central molecule. It might be possible that a molecule, which is considered for q_4 calculation, does not take part in the hydrogen bonding due to its not satisfying any of the hydrogen-bonding (HB) criteria and vice versa. Thus, we need to check if a central molecule forms n hydrogen bonds, i.e., $C_{HB=n}$, whether all these n molecules are also the first n nearest neighbors. For that, we have calculated a factor, P_{CNHB}, defined as P_{CNHB} = [number of water molecules attached to central molecule via HB]/[number of above hydrogen-bonded molecules that fall within n nearest neighbor molecules from the central molecule]. This factor is calculated to be close to unity for all $C_{HB=n}$ throughout the temperature range. Hence, we can consider that, in the case of $C_{HB=n}$, these n-hydrogen-bonded molecules are also the first n nearest neighbors with respect to the central molecule.

In order to investigate the effect of hydrogen bonding on the relative radial arrangement of water molecules, we have calculated oxygen−oxygen radial distribution functions (RDFs) with the restriction that the central molecule is n-hydrogen-bonded (for n = 2−5). It is important to note that there is no restriction in choosing neighboring molecules around the central molecule. These RDFs are shown in Figure 5b, and it is found that features of the RDF are very much influenced by the number of hydrogen bonds the central molecule is attached with. First of all, irrespective of the value of n, $g(r)$ plots show a well-defined shell structure. Moreover,

dx.doi.org/10.1021/jp404478y | J. Phys. Chem. B 2013, 117, 8831−8843

integration of $g(r)$ up to a distance corresponding to the first minimum of $g(r)$ yields nearly n number of molecules for $C_{HB=n}$, confirming that $C_{HB=n}$ has n nearest neighbors, all of which are H-bonded to the central molecule and thus they form the first shell for this central molecule. Now, in order to check further whether we can really define the first shell by considering only these n-H-bonded neighbors of a central molecule, we have calculated average distances of the nth and $(n + 1)$th molecules when the central molecule is n-hydrogen-bonded, i.e., for $C_{HB=n}$. In Figure 6a, we have shown the

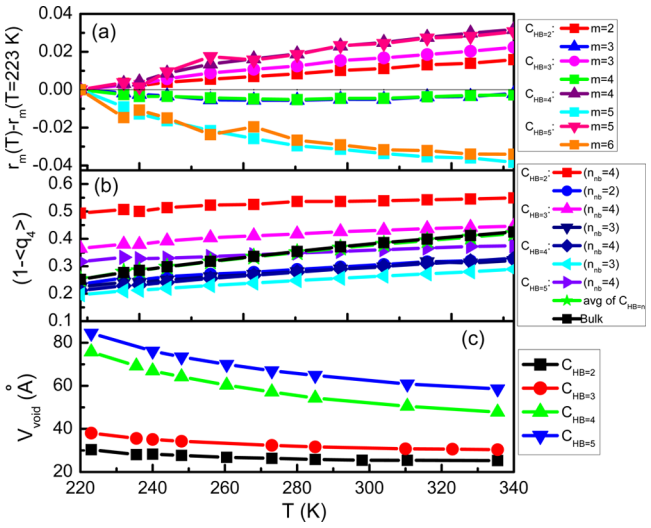

Figure 6. (a) Average distance r_n of the nth nearest neighbor at a temperature T relative to its distance at T = 223 K from the central molecule $C_{HB=n}$. The thin black horizontal line in the middle is a demarcation line between those with expansion and contraction. (b) Deviation of the tetrahedral order parameter q_4 from an ideal tetrahedral value of 1 as calculated for a central molecule $C_{HB=n}$ by considering the usual definition of four nearest neighbors as well as n nearest neighbors as a function of temperature. (c) Volume of the void space between the first and second solvation shell of a central water molecule $C_{HB=n}$, the solvation shell of which is defined by considering n water molecules (not four) as a function of temperature.

distance r_n or r_{n+1} relative to the same at T = 223 K to check whether it has expanded or shrunk at a temperature T relative to its value at T = 223 K. It is interesting to observe that the average distance of the nth molecule is gradually increasing, while that of the $(n + 1)$th molecule is decreasing with increasing temperature, irrespective of the value of n. In other words, the nth molecule (with respect to its position at T = 223 K) moves outward from the central molecule and the $(n + 1)$th molecule moves inward toward the central molecule as the temperature increases. This is even true for $C_{HB=5}$ and cannot be explained on the basis of the conventional definition of the first shell with four neighboring molecules. By conventional definition, for $C_{HB=5}$, both fifth and sixth molecules should be in the second shell and therefore their distances from the central molecule should have identical temperature dependence. However, we found that fifth and sixth molecules behave in opposing fashion in this case as the temperature is raised. In summary, we have found that, for a central molecule $C_{HB=n}$, the nth water molecule always expands whereas the $(n + 1)$th molecule contracts with respect to the central molecule. Thus, whether the distance of any nearest neighbor molecule from the central one would increase or decrease with the increase of temperature is dependent on the value of n for $C_{HB=n}$ (i.e., the number of hydrogen-bonded neighbors the central molecule possesses). For example, if the central molecule has two hydrogen bonds, then the distance of the second (nth) molecule from the central one will increase and that of the third ($(n + 1)$th) molecule will decrease. This general picture is clearly observed in Figure 6a. Thus, we can define the first shell of a molecule on the basis of the number of hydrogen-bonded neighbors the central molecule has. As we have already observed (see Figure 5a), water consists of various $C_{HB=n}$ molecules; therefore, water can be viewed as a broken H-bonded network with different n-hydrogen-bonded (n = 1−6) molecules with their distinct solvation shells. The radial position of nth and the $(n + 1)$th molecules can then be regarded as the outer boundary of the first shell and the inner boundary of the second shell, respectively, of a central molecule $C_{HB=n}$.

Besides translational correlation, we have also investigated the effect of H-bonded and non-H-bonded neighbors on the orientational order of the nearest neighbor molecules around a central molecule. In this case also, we have classified molecules into different groups according to the number of hydrogen-bonded neighbors it has. For calculating the tetrahedral order parameter, q_4, of a central molecule with $C_{HB=n}$, we have considered two definitions. In one case, the usual definition with four neighboring molecules has been considered, and in the other case, a modified definition by considering only n nearest neighbors (those H-bonded) to the central molecule $C_{HB=n}$ has been considered (see the Models and Methods section). The modified equation has been used in the case of $C_{HB=2}$ and $C_{HB=3}$, but for $C_{HB=5}$, we have used a conventional definition with only four neighbors. In Figure 6b, we have shown the deviation $(1 - \langle q_4 \rangle)$ of the q_4 values from the perfectly tetrahedral value of 1 as calculated for different groups of molecules as a function of temperature. It is interesting to observe that, in general, the deviation is larger in the case of $C_{HB=n}$ for n not equal to 4. For example, if the number of neighboring molecules (n_{nb}) considered is greater than n (no. of hydrogen-bonded neighbors), then the deviation is larger as compared to the cases when we take $n_{nb} = n$ in calculating q_4. It is observed that the deviation from the tetrahedral value of 1 is more for the red line with squares (for which we have considered $n_{nb} > n$) than that for the blue line with circles (for which we have considered $n_{nb} = n$) for the central molecule $C_{HB=2}$, and also the magenta line with up-triangles ($n_{nb} > n$) has more deviation than the orange line with down-triangles ($n_{nb} = n$) for the central molecule $C_{HB=3}$. Therefore, it turns out that, if we consider the conventional solvation shell with four neighboring molecules, it is the non-hydrogen-bonded (to the central molecule) neighbor that causes the deviation in tetrahedral order and induces asymmetry in local water structure. It was shown earlier by using the conventional definition of q_4 that $C_{HB=2}$ and $C_{HB=3}$ molecules are associated with the low-q_4 peak in the distribution of the tetrahedral order parameter.[28] However, the origin of this deviation is not clearly understood. When we compare q_4 values calculated by using only n neighboring molecules of $C_{HB=n}$, with n = 2−4 (i.e., for the cases $C_{HB=2}$, n_{nb} = 2, $C_{HB=3}$, n_{nb} = 3, $C_{HB=4}$, n_{nb} = 4), we have found the deviation (see lines with blue circles, orange down-triangles, and dark blue diamonds) to be less and quite close to each other. If we consider even the first three neighbors for $C_{HB=4}$, or first two neighbors of $C_{HB=3}$, the tetrahedral order parameter does not change very much. It clearly shows that all

dx.doi.org/10.1021/jp404478y | J. Phys. Chem. B 2013, 117, 8831−8843

hydrogen-bonded neighbors are preferentially occupying tetrahedral angular positions around a central molecule throughout the temperature range, irrespective of n of the central molecule. Only in the case $C_{HB=5}$, although all four neighboring molecules (considered for q_4 calculation) are H-bonded, the deviation is slightly more than all other $C_{HB=n}$ calculated with $n_{nb} \leq n$. In this case, since the central molecule is H-bonded with five neighboring molecules, due to geometrical restriction, all five molecules cannot be perfectly tetrahedrally coordinated, and therefore, any two neighbors with the central molecule make an angle different from the tetrahedral angle. In general, non-hydrogen-bonded molecules possess a lower symmetry and occupy sites other than tetrahedral. The present result thus reveals that the steady decrease of q_4 values or increase of the deviation (using the usual definition of four nearest neighbors) with temperature should not be attributed to distortion of tetrahedral symmetry of all the neighboring molecules; instead, it is a result of increasing proportion of non-hydrogen-bonded molecules (having non-tetrahedrally coordinated to the central molecule) in the first shell at higher temperatures. As the percentage of molecules with $C_{HB=2}$ and $C_{HB=3}$ increases with temperature, non-hydrogen-bonded molecules also increase, leading to more distortion in tetrahedral arrangements. It was shown[16] earlier that distortion in tetrahedral structure is one of the factors responsible for the anomalous density trend of water. However, how these distortions occur with respect to the local structure of water was not clear. Present observation is very significant to understand the molecular arrangement of the first shell, where the first shell is defined by the nearest four molecules. It is now clear that, among the four molecules in the conventional first shell, some molecules that are H-bonded to the central molecule show entirely different structural properties (mostly occupying tetrahedral positions) from those not H-bonded to the central molecules (inducing distortion to the tetrahedral arrangements). In this figure, we have also shown the deviation values (black squares) of bulk water as calculated from the usual definition involving four neighboring molecules and those calculated by considering a new definition of the solvation shell considering only n-hydrogen-bonded neighbors weighted by the respective proportions of $C_{HB=n}$. It is interesting to observe that these two results are in excellent agreement. Thus, the results presented in Figure 6b further confirm that the structure of a solvation shell of a molecule depends on the H-bonding characteristic of the central molecule and reinforces the view that water can be considered as a normal H-bonded liquid with broken hydrogen bonds having different proportions of n-hydrogen-bonded water molecules with distinct newly defined solvation shells.

It was shown in an earlier study[16] that the density anomaly is a result of two linear correlations: the homogeneous expansion of oxygen−oxygen distance and contraction due to angular distortion against temperature. These two opposing correlations can now be easily understood by analyzing the results of Figures 5 and 6. In Figure 6a, we have found that, for a central molecule $C_{HB=n}$, the distance of the nth neighbor increases but that of the $(n + 1)$th neighbor, which is not hydrogen-bonded to the central molecule (and therefore causes more angular distortion), contracts (cf. Figure 6b) with respect to the central molecule as the temperature increases. Thus, the present results not only corroborate the findings of earlier work[16] but also pinpoint the exact mechanism by which expansion and contraction occurs. It can be further illustrated from Figure 5b, in which it is shown that for $C_{HB=n}$ with $n = 4$ and 5, the first two peaks are well separated with a deep minimum between the two, but for $C_{HB=n}$ with $n = 2$ and 3, where there are non-hydrogen-bonded neighbors (for which angular distortion is more), the first two peaks are very close to each other. In order to corroborate this picture, in Figure 6c, we have shown the void volume associated with the solvation shell of a central molecule $C_{HB=n}$, where the void volume is defined as the space available between two concentric spheres of radii r_{n+1} and r_n around the central molecule $C_{HB=n}$. It is interesting to observe that, at all temperatures, the void volume between the (newly defined) first and the second shells for the central molecule $C_{HB=n}$ with $n = 4$ or 5 is much more than that for $n = 2$ or 3. It is also evident (see Figure 6c) that void volume decreases with increasing temperature in all the cases and the rate of decrease is n-dependent. How this change in void volume with temperature contributes to the density anomaly of water has been discussed later.

The distribution of q_4 at a lower temperature is unimodal with a single peak (at a q_4 value close to 1) corresponding to an almost tetrahedral configuration, and as the temperature is increased, another peak develops at a lower q_4 value of around 0.5 (see inset of Figure 7b). It is intriguing to observe that this

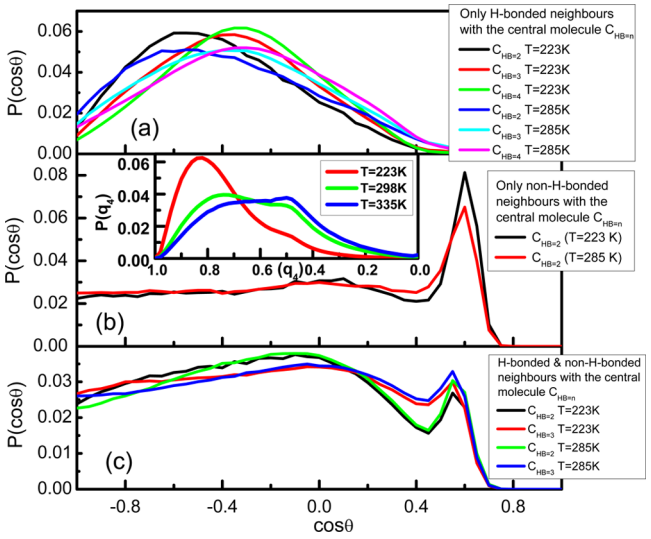

Figure 7. Distributions $P(\cos\theta)$ of the cosine of angle θ made by (a) two hydrogen-bonded, (b) two non-hydrogen-bonded, and (c) one hydrogen-bonded and the other non-hydrogen-bonded nearest neighbors to the central molecule $C_{HB=n}$. In the inset of panel b, we have shown the distributions of tetrahedral order parameters q_4 for three different temperatures.

new peak appears at a particular q_4 value only. As we know that elevation of temperature in general increases randomness, which can flatten the distribution, it should not prefer any preferred angular arrangement. Therefore, the development of a new peak corresponding to a particular angular orientation (represented by a value of $q_4 = 0.5$) at a higher temperature is quite puzzling. The usual calculation of q_4 takes into account angular arrangements of the nearest four molecules from the central one. We have already shown (cf. Figure 6b) that the neighbors that are not hydrogen-bonded to the central molecule induce more deviation from the tetrahedral arrangement than those H-bonded to the central molecule. In order to understand the origin of the new peak (see inset of Figure 7b)

dx.doi.org/10.1021/jp404478y | J. Phys. Chem. B 2013, 117, 8831−8843

in the distribution $P(q_4)$ at a higher temperature, we have further analyzed angular arrangements of the neighboring molecules around a central molecule $C_{HB=n}$ (i.e., the central molecule having n-H-bonded neighbors). We have classified angle θ_{jik} (where i is the central molecule and j and k are any two of its nearest neighbors) into three groups: (1) both j and k are hydrogen-bonded to the central molecule i, (2) j and k, both are non-hydrogen-bonded to the central molecule i, and (3) only one of j and k is hydrogen-bonded with the central molecule i. We have used the distribution of $\cos\theta$ instead of q_4 (in order to get rid of the square of the $\cos\theta$ term in the q_4 equation) to get a clearer picture of the angular arrangement. When we consider category 1 stated above, we found a unimodal distribution of $\cos\theta$ (see Figure 7a), with only one peak corresponding to an almost tetrahedral angle. Also, it has been found that the peak position of the distribution does not change much with temperature. This observation is in accordance with the outcome of Figure 6b, which shows a very small change in the q_4 values with the increase in temperature, provided only hydrogen-bonded molecules have been taken into account for the q_4 calculation. Category 2 above is possible when the central molecule is hydrogen-bonded to only two of its neighbors, i.e., $C_{HB=2}$ (so that in the conventional solvation shell of four neighbors, the central molecule has two non-hydrogen-bonded neighbors). Existence (see Figure 7b) of only one sharp peak at around $\cos\theta = 0.6$ corresponding to the q_4 value of around 0.5 (i.e., $\theta = 53-60°$) has been observed. In the third category, the angle we consider is extended at the central molecule by one neighbor, which is hydrogen-bonded and the other one, which is not H-bonded to the central molecule. In this case (see Figure 7c), it is further surprising to find that, apart from the sharp peak at around $\cos\theta = 0.6$, a new broad peak appears at around $\cos\theta = 0$ in the distribution. The development of this new angular arrangement (corresponding to $\cos\theta = 0.0$) makes the analysis further complicated.

If we consider a usual definition of first shell, then we have one central molecule surrounded by four neighbors. Here we have calculated the total number of hydrogen bonds formed among these five molecules (one central molecule and its four nearest neighbors). In this calculation, H-bonding of the first shell neighbors with the molecules from the second shell has not been considered. We have found four hydrogen bonds inside the conventional first shell for $C_{HB=n}$ irrespective of the value of n. It is also observed that, in the case of $C_{HB=4}$, the central molecule is involved in all four hydrogen bonds with no interneighbor hydrogen bond between any two of the neighboring molecules. For $C_{HB=3}$ and $C_{HB=2}$, there are respectively three and two hydrogen bonds involving the central molecule and the neighbors. Therefore, the remaining hydrogen bond/s (one for $C_{HB=3}$ and two for $C_{HB=2}$) is/are resulting from the interneighbor hydrogen bonding involving two neighboring molecules only (i.e., no involvement of the central molecule). We have further investigated how this hydrogen bond, which is not associated with the central molecule, is formed. In the case of $C_{HB=3}$, we have found that this hydrogen bond is actually between the fourth neighbor, which is non-hydrogen-bonded to the central molecule and any one of the rest of the three neighbors that is already hydrogen-bonded to the central molecule. Whether the fourth non-hydrogen-bonded (to the central molecule) neighbor has any preference for selecting (for hydrogen bond formation) one among the three neighbors (those hydrogen-bonded to the central molecule) has also been investigated. The probability of forming a hydrogen bond by the fourth non-hydrogen-bonded (to the central molecule) neighbor with any of the three other neighbors (that are centrally hydrogen-bonded) has been found to be ~0.33. Therefore, all three centrally hydrogen-bonded neighbors are equally probable to form this H-bond with the fourth molecule, which is not hydrogen-bonded with the central one. This observation that all three hydrogen-bonded neighbors are equally susceptible to form a H-bond with the fourth centrally non-hydrogen-bonded neighbor supports our hypothesis that the first solvation shell can be defined according to the number of hydrogen bonds the central molecule is having. In the case of $C_{HB=2}$, out of a total of four H-bonds in the first shell, two involve the central molecule and the remaining two hydrogen bonds are among the neighbors (no involvement of the central molecule). In this case, two non-hydrogen-bonded (to the central molecule) neighbors always form a H-bond between them (probability is 1) and another hydrogen bond is formed between a centrally H-bonded neighbor and any one of the two (equally probable) centrally non-hydrogen-bonded neighbors (calculated probability is around 0.5).

As has been discussed earlier, in the case of $C_{HB=3}$, three molecules have occupied three tetrahedral positions. It is expected that the fourth neighbor, the non-hydrogen-bonded one, would approach from the side where there is a vacant tetrahedral site. However, in that case, the angle formed by this neighbor with the central one and any other neighbor in the first solvation shell would have been close to a tetrahedral angle of around 109°. However, we found (see Figure 7c) two peaks, one at $\cos\theta = 0.6$ corresponding to a small angle of around 50−60° and another at around $\cos\theta = 0.0$ corresponding to an angle of around 90°. Therefore, this fourth molecule approaches the central molecule from the opposite side of the vacant tetrahedral site in such a way that it forms a right angle with the two neighbors and forms a hydrogen bond with the remaining one. This situation has been shown schematically in Figure 8. The fourth molecule comes along the diagonal plane containing the third neighbor and the central molecule from the side of the third neighbor with which it forms a hydrogen bond (the red line representing a hydrogen bond between the two neighbors designated by 3 and 4 in Figure 8) and thus makes a smaller angle ($\cos\theta \approx 0.6$) with the central molecule and the third neighboring molecule. In the process, it forms two other angles corresponding to about $\cos\theta \approx 0.0$ (right angle), with the first and second neighboring water molecules (that reside on the other diagonal plane of the cube) involving the central molecule (see Figure 8). Angles related to $C_{HB=2}$ shown in Figure 7c can also be explained in the same manner. In summary, the appearance of the main peak in the q_4 distribution at around $q_4 = 1$ originates (see inset of Figure 7b) from those neighbors that form H-bonds directly with the central molecule, whereas the second peak of $P(q_4)$ at a higher temperature can be attributed to the formation of interneighbor hydrogen bonds. This situation arises only in the cases of $C_{HB=2}$ and $C_{HB=3}$. As the fraction of molecules having $C_{HB=2}$ and $C_{HB=3}$ and therefore the population of the non-hydrogen-bonded (to the central molecule) neighbors increases with temperature, the intensity of the second peak (at $q_4 = 0.5$) increases accordingly.

Then, we have looked into the anomalous density trend of water in light of this new definition of the first shell based on $C_{HB=n}$. We have already seen that, with the increase in temperature, the distance of the nth molecule from the central

dx.doi.org/10.1021/jp404478y | J. Phys. Chem. B 2013, 117, 8831−8843

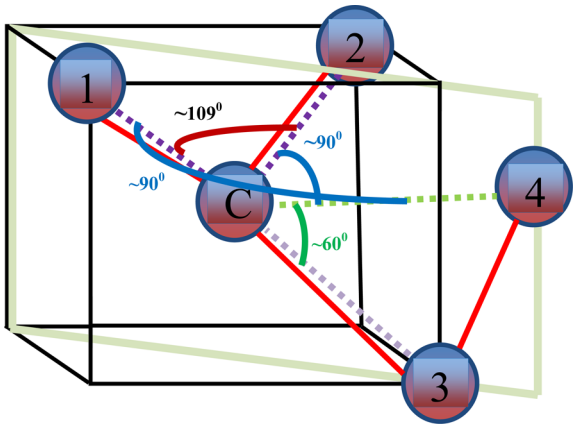

Figure 8. A schematic representation (not to scale) of a central molecule C, which is hydrogen-bonded to three water molecules in the conventional first shell. The hydrogen bonds have been shown by red lines, whereas dashed lines are to guide the eye for measuring angles among the neighbors with the central molecule. The fourth molecule is approaching the central molecule along the diagonal plane (shown by the light green parallelogram) in such a way that it makes 90° angles with two (residing on the other diagonal plane of the cube and designated as 1 and 2 in the picture) of the three hydrogen-bonded (to the central one) neighbors. It also makes a small angle of around 60° with the third H-bonded neighbor (designated as 3) and forms a hydrogen bond with the third neighbor. Energetic cost due to steric hindrance for the formation of such a small angle instead of a tetrahedral angle is probably compensated by the gain in energy due to H-bond formation between the neighbors 3 and 4.

molecule $C_{HB=n}$ (i.e., the radius of the newly defined first shell) increases, whereas the inner boundary of the second shell (as defined by the distance of the $(n + 1)$th molecule from the central molecule $C_{HB=n}$) approaches toward the center. Thus, the void space between the first and second shells reduces with temperature. It is important to note[15] that the region up to the second minimum of the radial distribution function $g_{OO}(r)$ contains all the information related to density or volume. We have divided this region into three parts, (i) the first shell as defined by the newly defined solvation shell according to the number of H-bonds associated with the central molecule, (ii) the void space, i.e., the space between the outer boundary of the first shell (of radius r_n) and the inner boundary of the second shell (distance from the central molecule is r_{n+1}), and (iii) the second shell. As usual, we have assumed that both of the shells are spherical in nature. For the calculation of orientational order parameters (q_4 and Q_6), conventionally, the positions of the 4th and 16th molecules are considered to be the outer boundaries of the first and second shells, respectively. As we have defined the first shell in a different way (by taking n neighbors around a central molecule $C_{HB=n}$), the outer boundary of the second shell also needs to be redefined. For that, we have computed the number of molecules in the second shell by integrating (see inset of Figure 5b) the RDF for all $C_{HB=n}$, where lower and upper limits of integration have been chosen accordingly from the troughs of the respective RDF. It is found that, irrespective of the nature of the central molecule (i.e., value of n in $C_{HB=n}$), the number of molecules in the second shell varies between 19.5 and 20.5. We have also calculated the average distance of the 16th molecule for each central molecule $C_{HB=n}$, and we have found $\langle r_{16} \rangle$ to be around 4.8 Å, which is close to the upper integration limit chosen in the above-mentioned integration. Then, we have calculated the volume or density by considering the kth molecule as the boundary of the second shell, where k varies from 16 to 20 and we have found that there is almost no significant change in volume/density trend for these different k values. Therefore, we have considered the position of the 16th molecule as the outer boundary of the second second shell for our volume/density calculation. The volume of the second shell has been calculated by subtracting the volume of a smaller sphere of radius r_{n+1} from that of a larger sphere of radius r_{16}, where r_{n+1} and r_{16} represent the positions of the $(n + 1)$th and 16th neighbors, respectively, of a central molecule $C_{HB=n}$. Similarly, the volume of the void space between the first and second shells has been calculated by subtracting the volume of a smaller sphere of radius r_n from that of a larger sphere of radius r_{n+1}.

In Figure 9a, we have shown the average volume of the first and second shells and the void volume between the two shells

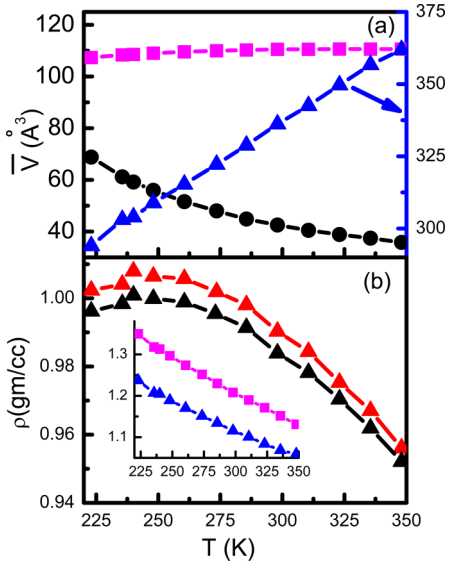

Figure 9. (a) Volumes of the first shell (magenta squares), the second shell (blue triangles), and the void space between the two shells (black circles) of SPC/E water as a function of temperature. The blue curve follows the scale on the right axis, whereas the magenta and black curves follow that on the left axis. (b) Density ρ in g/cc of SPC/E water as a function of temperature. The red line with triangles represents the density of water in the second shell including the void space between the two shells. The black line with triangles represents the average bulk density of water. Inset: The magenta line with squares represents the density of the first shell, whereas the blue line with triangles represents the density of only the second shell (without the void space).

separately. Since, in our definition of the first shell, the number of neighbors is not fixed (dependent on the number of H-bonds of the central molecule), the volume of the first shell is calculated as $\overline{V} = \sum_{n=1}^{5} V_n f_n$, where $V_n = (4\pi/3) r_n^3$ and f_n is the fraction of molecules having n hydrogen bonds. As shown in Figure 9a, the volume of the first as well as second shell increases with an increase in temperature. This expansion of the first shell has already been shown in Figure 6a, where the average distance of the nth neighbor of a central molecule $C_{HB=n}$ having n hydrogen bonds increases with increasing temperature. And it is true for any n. The change in volume of the first shell with temperature is not much; i.e., the first shell is quite incompressible. It is important to note that, unlike these two shells, the volume of the void space between the two shells

dx.doi.org/10.1021/jp404478y | J. Phys. Chem. B 2013, 117, 8831−8843

decreases (see Figure 9a, black curve) with temperature. We have also calculated the density of these different regions corresponding to the first shell and second shell. During density calculation, we have to remember that the numbers of molecules in the first and second shells vary according to the value of n of the central molecule $C_{HB=n}$. We have also calculated the density of the second shell by incorporating the void space into the second shell (i.e., starting from the nth to 16th molecules). The following equation has been used for the calculation of densities in different regions:

$$\rho = \frac{\sum_{n=1}^{5} N_n f_n}{\bar{V}}$$

where ρ is the average density and N_n and f_n are the number of molecules inside the given volume $\bar{V}$ and the fraction of molecules with n hydrogen bonds, respectively. For example, for the first shell $N_n = n + 1$ (n-hydrogen-bonded neighbors and the central molecule) and for the second shell $N_n = 16 - n$. As shown in Figure 9b, the densities of first and second shells monotonically decrease with increasing temperature and thus cannot explain the density maximum of water. Elevation of temperature leads to an increase in oxygen−oxygen distance and volume. That is why we observe a decrease of densities of the first and second shells. However, when we consider the density of the second shell by incorporating the void space between the first and second shells, it increases first and then decreases with increasing temperature. Thus, it can describe the non-monotonic density trends with respect to temperature. The location of the TMD (T_{TMD} = 240 K for the SPC/E model) and the overall trend of the temperature dependence of the average bulk density have been reproduced correctly. Thus, the second shell including the void space is the responsible region for the density anomaly. The importance of the second shell in explaining the anomalous density trend has been noted earlier.[15] A molecular theory of liquid water also highlights[52] the importance of longer-than-near-neighbor-ranged interactions. It clearly states that a detailed treatment of local order alone corresponding only to the tetrahedral local structure without invoking the effect of longer ranged interaction cannot describe the thermodynamic properties of network forming liquid like water. We have already shown that the structure of the first shell is very much governed by $C_{HB=n}$. With the increase in temperature, thermal expansion is always there, but it is the void volume that determines the anomalous expansion of water and this void volume decreases as the percentage of $C_{HB=4}$ gradually decreases and that of $C_{HB=2}$ or $C_{HB=3}$ increases. It is because the void volume associated with $C_{HB=2}$ as well as $C_{HB=3}$ is much less as compared to the same associated with $C_{HB=4}$ and $C_{HB=5}$. And as the angular distortion associated with $C_{HB=2}$ or $C_{HB=3}$ is more, the overall distortion also increases with the increase in temperature.[16] Thus, in essence, water can be viewed as a normal dynamic mixture of different solvation shells defined according to the number of hydrogen-bonded neighbors of the central molecule. The temperature dependence of the behavior of all these solvation shells is distinctly different. The hydrogen bonding status of the central molecule governs not only the property of the first shell but that of the second shell and the void space also. The anomalous density change of water with temperature can then be attributed to the change in the proportions of these different solvation shells (i.e., hydrogen bond distribution) by properly taking into account the density change in the region of the second shell and the void space between the first and second shells.

CONCLUSIONS

We show that the hydrogen bonding network structure dictates structural orders and anomalies of water. In particular, the average number of hydrogen bonds correlates well not only with tetrahedral and second shell's orientational orders but with the structure factor and the density anomaly of water as well. Thus, disparate results on the temperature dependence of various structural orders and TMD as obtained from different water models have been concurred by correlating these results in terms of the average number of hydrogen bonds. Our result is consistent with the recent observation[23] that all water models follow the same structural pattern by a temperature shift. This is understandable because a shift in temperature changes the average number of hydrogen bonds. An in-depth analysis of the H-bond network of the water molecules reveals that the solvation shell of a water molecule can be defined not by the average number of four neighbors but by the number of hydrogen-bonded neighbors of the central molecule. It has been observed that, for a central molecule $C_{HB=n}$, the distance of the nth molecule from the central molecule always increases and that of the $(n + 1)$th molecule always decreases with the increase in temperature. This result is consistent with the findings of Matsumoto,[16] who observed that the density anomaly is a result of interplay of the monotonic oxygen−oxygen distance extension and angular distortion of the tetrahedral network upon change of temperature. However, the origin of the angular distortion in the tetrahedral network was not clear. In this investigation, we put forward a lucid explanation of the relation of tetrahedral distortion and volume contraction against temperature. First, we have shown that the distortion arises from those water molecules that are not directly hydrogen-bonded to the central molecule. All the hydrogen-bonded (to the central molecule) neighbors occupy tetrahedral positions around the central molecule even at higher temperatures and therefore have minimal angular distortion. It is the non-hydrogen-bonded (to the central molecule) neighbor which induces distortion in the tetrahedral arrangement. We have also identified the origin of the appearance of the second peak in the distribution of tetrahedral order parameters at higher temperatures. This second peak appears due to the asymmetrical approach of a non-hydrogen-bonded neighbor toward the central molecule in such a way (see Figure 8) that it forms a hydrogen bond with another neighbor, which is already hydrogen-bonded to the central molecule. Because of this hydrogen bond formation between the non-hydrogen-bonded neighbor with the other neighbor, which is already hydrogen-bonded to the central molecule of the type $C_{HB=2}$ or $C_{HB=3}$, the angle extended by these two neighbors to the central molecule is much smaller (see the peaks at $\cos\theta = 0.6$ and 0.0 in Figure 7b and c) than the usual tetrahedral angle of around 109° (see Figure 8). Our result is consistent with the recent work of Netz and co-workers,[31] who have shown that the additional peaks at low q_4 values arise from the two- and three-hydrogen-bonded molecules. However, it is important to note that not all four neighbors of a two- or three-hydrogen-bonded water molecule (designated as $C_{HB=2}$ or $C_{HB=3}$ here) are orientationally distorted. In fact, we have found that all the neighbors that are hydrogen-bonded to the central molecule (irrespective of the hydrogen bonding status of the central molecule) are (almost) tetrahedrally coordinated to the central molecule, and

dx.doi.org/10.1021/jp404478y | J. Phys. Chem. B 2013, 117, 8831−8843

it is the non-hydrogen-bonded neighbor (one in the case of $C_{HB=3}$ and two in the case of $C_{HB=2}$) that distorts the tetrahedral angular arrangement. The present result therefore contradicts a recent finding[34] in which water has been viewed as a mixture of two components based on the median of the q_4 values. Finally, we have correlated this tetrahedral distortion with volume contraction in the following way. The volume of the void space (space between the first and second shells) associated with the central molecule having four tetrahedral neighbors is much more than the same associated with a central molecule having one or more non-tetrahedral neighbors (those cause more angular distortion), and the decrease of void volume against temperature in the former case is more as compared to that in the later case (see Figure 6c). We have finally found that the volume of the void space between the first and second shells of a central molecule along with that of the second shell collectively determines the anomalous density trend of water. An experimental result[25] on water structure also predicts that density change in water is associated with the structural change in the second coordination shell. If we consider water as a dynamic mixture of various solvation shells of *n*-hydrogen-bonded (with $n = 2-5$) water molecules, the volume of the second shell along with the void space between the first and second shells of this mixture follows the correct non-monotonic density change with temperature and therefore explains the density anomaly of water (see Figure 9). It is important to emphasize that this mixture is not made up of any spatially correlated extended clusters of molecules, as posited by Huang et al.[28] to interpret their small angle structure factor data and also not consisting of orientationally correlated clusters[34] of water molecules having a range of q_4 values. Rather, as the present investigation suggests, water can be viewed as a temporal mixture of differently hydrogen-bonded water molecules, with the composition of this mixture being instantaneously changing due to thermal motion. The density anomaly of water is a consequence of neither spatial nor orientational polyamorphism but a result of natural fluctuations[29,30] of hydrogen-bonded network arising due to usual stochastic processes in a single component fluid. The present result is consistent with the experimental finding of Smith et al.[40] that shows that the distributions of hydrogen bonding geometries and energies in liquid water are continuous and that of Head-Gordon et al.[42] that describes water as a tetrahedral hydrogen-bonded network. In summary, our finding is in contradiction to the assumption of density heterogeneity made in refs 28 and 34 and in line with the view that liquid water is a random network of hydrogen bonds, with fleetingly broken bonds, that is perpetually undergoing topological reorganization as inferred in refs 16, 29, 31, 36, 40, and 42.

AUTHOR INFORMATION

Notes

The authors declare no competing financial interest.

ACKNOWLEDGMENTS

It is a pleasure to thank Dr. S. K. Sarkar for his support and encouragement and Dr. T. Bandyopadhyay for GROMACS related help. We also thank Computer Division, BARC, for providing supercomputing facilities and support.

REFERENCES

(1) Franks, F. *Water. A Comprehensive Treatise*; Plenum: New York, 1973.
(2) Dill, K.; Truskett, T.; Vlachy, V.; Hribar-Lee, B. Modeling Water, the Hydrophobic Effect, and Ion Solvation. *Annu. Rev. Biophys. Biomol. Struct.* **2005**, *34*, 173−199.
(3) Ball, P. Water as an Active Constituent in Cell Biology. *Chem. Rev.* **2008**, *108*, 74−108.
(4) Bellissent-Funel, M.-C. *Hydration Processes in Biology: Theoretical and Experimental Approaches*; IOS Press: Amsterdam, The Netherlands,1999.
(5) Ludwig, R. Water: From Clusters to the Bulk. *Angew Chem. Int. Ed.* **2001**, *40*, 1808−1827.
(6) Angell, C. A.; Shuppert, J.; Tucker, J. C. Anomalous Properties of Supercooled Water. Heat Capacity, Expansivity, and Proton Magnetic Resonance Chemical Shift from 0 to −38°. *J. Phys. Chem.* **1973**, *77*, 3092−3099.
(7) Kell, G. S. Density, Thermal Expansivity and Compressibility of Liquid Water from 0° to 150°C: Correlations and Tables for Atmospheric Pressure and Saturation Reviewed and Expressed on 1968 Temperature Scale. *J. Chem. Eng. Data* **1975**, *20*, 97−105.
(8) Saul, A.; Wagner, W. A Fundamental Equation for Water Covering the Range from the Melting Line to 1273 K at Pressures up to 25000 MPa. *J. Phys. Chem. Ref. Data* **1989**, *18*, 1537−1564.
(9) Speedy, R. J.; Angell, C. A. Isothermal Compressibility of Supercooled Water and Evidence for a Thermodynamic Singularity at −45°C. *J. Chem. Phys.* **1976**, *65*, 851−858.
(10) Angell, C. A.; Bressel, R. D.; Hemmati, M.; Sare, E. J.; Tucker, J. C. Water and Its Anomalies in Perspective: Tetrahedral Liquids with and without Liquid-Liquid Phase Transitions. *Phys. Chem. Chem. Phys.* **2000**, *2*, 1559−1566.
(11) Errington, J. R.; Debenedetti, P. G. Relationship between Structural Order and the Anomalies of Liquid Water. *Nature* **2001**, *409*, 318−321.
(12) Mishima, O.; Stanley, H. E. The Relationship between Liquid, Supercooled and Glassy Water. *Nature* **1998**, *396*, 329−335.
(13) Kumar, P.; Buldyrev, S. V.; Stanley, H. E. A Tetrahedral Entropy for Water. *Proc. Natl. Acad. Sci. U.S.A.* **2009**, *106*, 22130−22134.
(14) Giovambattista, N.; Stanley, H. E.; Sciortino, F. Phase Diagram of Amorphous Solid Water: Low-Density, High-Density, and Very-High-Density Amorphous Ices. *Phys. Rev. E* **2005**, *72*, 031510-1−031510-12.
(15) Yan, Z.; Buldyrev, S. V.; Kumar, P.; Giovambattista, N.; Debenedetti, P. G.; Stanley, H. E. Structure of the First- and Second-Neighbor Shells of Simulated Water: Quantitative Relation to Translational and Orientational Order. *Phys. Rev. E* **2007**, *76*, 051201-1−051201-5.
(16) Matsumoto, M. Why Does Water Expand When It Cools? *Phys. Rev. Lett.* **2009**, *103*, 017801-1−017801-4.
(17) Nayar, D.; Agarwal, M.; Chakravarty, C. Comparison of Tetrahedral Order, Liquid State Anomalies, and Hydration Behaviour of mTIP3P and TIP4P Water Models. *J. Chem. Theory Comput.* **2011**, *7*, 3354−3367 and references therein.
(18) Abascal, J. L. F.; Vega, C. A General Purpose Model for the Condensed Phases of Water: TIP4P/2005. *J. Chem. Phys.* **2005**, *123*, 234505-1−234505-12.
(19) Pi, H. L.; Aragones, J. L.; Vega, C.; Noya, E. G.; Abascal, J. L. F.; Gonzalez, M. A.; McBride, C. Anomalies in Water as Obtained from Computer Simulations of the TIP4P/2005 Model: Density Maxima, and Density, Isothermal Compressibility and Heat Capacity Minima. *Mol. Phys.* **2009**, *107*, 365−374.
(20) Horn, H. W.; Swope, W. C.; Pitera, J. W.; Madura, J. D.; Dick, T. J.; Hura, G. L.; Head-Gordon, T. Development of an Improved Four-Site Water Model for Biomolecular Simulations: TIP4P-Ew. *J. Chem. Phys.* **2004**, *120*, 9665−9678.
(21) Mahoney, M. W.; Jorgensen, W. L. A Five-Site Model for Liquid Water and the Reproduction of the Density Anomaly by Rigid, Nonpolarizable Potential Functions. *J. Chem. Phys.* **2000**, *112*, 8910−8922.
(22) Hansen, J.-P.; McDonald, I. *Theory of Simple Liquids*, 3rd ed.; Elsevier: New York, 2006.

(23) Shevchuk, R.; Prada-Gracia, D.; Rao, F. Water Structure-Forming Capabilities Are Temperature Shifted for Different Models. *J. Phys. Chem. B* **2012**, *116*, 7538−7543.
(24) Poole, P.; Sciortino, F.; Essmann, U.; Stanley, H. Phase Behaviour of Metastable Water. *Nature* **1992**, *360*, 324−328.
(25) Speedy, R. Stability-Limit Conjecture. An Interpretation of the Properties of Water. *J. Phys. Chem.* **1982**, *86*, 982−991.
(26) Stanley, H. E.; Teixeira, J. Interpretation of the Unusual Behaviour of H_2O and D_2O at Low Temperatures: Tests of a Percolation Model. *J. Chem. Phys.* **1980**, *73*, 3404−3422.
(27) Soper, A. K.; Ricci, M. A. Structure of High-Density and Low-Density Water. *Phys. Rev. Lett.* **2000**, *84*, 2881−2884.
(28) Huang, C.; Wikfeldt, K. T.; Tokushima, T.; Nordlund, D.; Harada, Y.; Bergmann, U.; Niebuhr, M.; Weiss, T. M.; Horikawa, Y.; Leetmaa, M.; Ljungberg, M. P.; Takahasi, O.; Lenz, A.; Ojamae, L.; Lyubartsev, A. P.; Shin, S.; Pettersson, L. G. M.; Nilsson, A. The Inhomogeneous Structure of Water at Ambient Conditions. *Proc. Natl. Acad. Sci. U.S.A.* **2009**, *106*, 15214−15218.
(29) Clark, G. N. I.; Hura, G. L.; Teixeira, J.; Soper, A. K.; Head-Gordon, T. Small-Angle Scattering and the Structure of Ambient Liquid Water. *Proc. Natl. Acad. Sci. U.S.A.* **2010**, *107*, 14003−14007.
(30) Soper, A. K.; Teixeira, J.; Head-Gordon, T. Is Ambient Water Inhomogeneous on the Nanometer-Length Scale? *Proc. Natl. Acad. Sci. U.S.A.* **2010**, *107*, E44-1.
(31) Sedlmeier, F.; Horinek, D.; Netz, R. R. Spatial Correlations of Density and Structural Fluctuations in Liquid Water: A Comparative Simulation Study. *J. Am. Chem. Soc.* **2011**, *133*, 1391−1398.
(32) Cuthbertson, M. J.; Poole, P. H. Mixturelike Behavior near a Liquid-Liquid Phase Transition in Simulations of Supercooled Water. *Phys. Rev. Lett.* **2011**, *106*, 115706-1−115706-4.
(33) English, N. J.; Tse, J. S. Density Fluctuations in Liquid Water. *Phys. Rev. Lett.* **2011**, *106*, 037801-1−037801-4.
(34) Overduin, S. D.; Patey, G. N. Understanding the Structure Factor and Isothermal Compressibility of Ambient Water in Terms of Local Structural Environments. *J. Phys. Chem. B* **2012**, *116*, 12014−12020.
(35) Xu, L.; Kumar, P.; Buldyrev, S. V.; Chen, S. H.; Poole, P. H.; Sciortino, F.; Stanley, H. E. Relation between the Widom Line and the Dynamic Crossover in Systems with a Liquid-Liquid Phase Transition. *Proc Natl. Acad. Sci. U.S.A.* **2005**, *102*, 16558−16562.
(36) Stillinger, F. H. Water Revisited. *Science* **1980**, *209*, 451−457.
(37) Wernet, Ph.; Nordlund, D.; Bergmann, U.; Cavalleri, M.; Odelius, M.; Ogasawara, H.; Naslund, L . Å.; Hirsch, T. K.; Ojamae, L.; Glatzel, P.; Pettersson, L. G. M.; Nilsson, A. The Structure of the First Coordination Shell in Liquid Water. *Science* **2004**, *304*, 995−999.
(38) Smith, J. D.; Cappa, C. D.; Wilson, K. R.; Messer, B. M.; Cohen, R. C.; Saykally, R. J. Enegetics of Hydrogen Bond Network Rearrangements in Liquid Water. *Science* **2004**, *306*, 851−853.
(39) Eaves, J. D.; Loparo, J. J.; Fecko, C. J.; Roberts, S. T.; Tokmakoff, A.; Geissler, P. L. Hydrogen Bonds in Liquid Water Are Broken Only Fleetingly. *Proc. Natl. Acad. Sci. U.S.A.* **2005**, *102*, 13019−13022.
(40) Smith, J. D.; Cappa, C. D.; Wilson, K. R.; Cohen, R. C.; Geissler, P. L.; Saykally, R. J. Unified Description of Temperature-Dependent Hydrogen Bond Rearrangements in Liquid Water. *Proc. Natl. Acad. Sci. U.S.A.* **2005**, *102*, 14171−14174.
(41) Luzar, A.; Chandler, D. Effect of Environment on Hydrogen Bond Dynamics in Liquid Water. *Phys. Rev. Lett.* **1996**, *76*, 928−931.
(42) Head-Gordon, T.; Johnson, M. E. Tetrahedral Structure or Chains for Liquid Water. *Proc. Natl. Acad. Sci. U.S.A.* **2006**, *103*, 7973−7977.
(43) Limmer, D. T.; Chandler, D. The Putative Liquid-Liquid Transition Is a Liquid-Solid Transition in Atomistic Models of Water. *J. Chem. Phys.* **2011**, *135*, 134503-1−134503-10.
(44) Jorgensen, W. L.; Chandrashekhar, J.; Madura, J. D.; Impey, R.; Klein, M. Comparison of Simple Potential Functions for Simulating Liquid Water. *J. Chem. Phys.* **1983**, *79*, 926−935.
(45) Neria, E.; Fischer, S.; Karplus, M. Simulation of Activation Free Energies in Molecular Systems. *J. Chem. Phys.* **1996**, *105*, 1902−1921.
(46) Berendsen, H. J. C.; Postma, J. P. M.; van Gunsteren, W. F.; Hermans, J. Interaction Models for Water in Relation to Protein Hydration; Pullman, B., Ed.; Reidel: Dordrecht, The Netherlands, 1981; pp 331−342.
(47) Berendsen, H. J. C.; Grigera, J. R.; Straatsma, T. P. The Missing Term in Effective Pair Potentials. *J. Phys. Chem.* **1987**, *91*, 6269−6271.
(48) Allen, M. P.; Tildesley, D. J. *Computer Simulation of Liquids*; Oxford University Press: New York, 1987.
(49) Van Der Spoel, D.; Lindahl, E.; Hess, B.; Groenhof, G.; Mark, A. E.; Berendsen, H. J. C. GROMACS: Fast, Flexible, and Free. *J. Comput. Chem.* **2005**, *26*, 1701−1718.
(50) Bandyopadhyay, D.; Mohan, S.; Ghosh, S. K.; Choudhury, N. Comparison of Orders, Structures and Anomalies of Water: A Molecular Dynamics Simulation Study. *AIP Conf. Proc.* **2013**, *1512*, 590−591.
(51) Huggins, D. J. Correlations in Liquid Water for the TIP3P-Ewald, TIP4P-2005, TIP5P-Ewald, and SWM4-NDP Models. *J. Chem. Phys.* **2012**, *136*, 064518-1−064518-13.
(52) Shah, J. K.; Asthagiri, D.; Pratt, L. R.; Paulaitis, M. E. Balancing Local Order and Long-Ranged Interactions in the Molecular Theory of Liquid Water. *J. Chem. Phys.* **2007**, *127*, 144508-1−144508-7.